Dynamic Replanning of Low Noise Rotorcraft Operations

Eric Greenwood
Aeroacoustics Branch
NASA Langley Research Center
Hampton, VA

ABSTRACT

A new method for rapidly planning and dynamically replanning low noise rotorcraft flight operations is developed. A large database of rotorcraft maneuver segments is generated, and an acoustic cost is assigned to each segment by using a computationally efficient semiempirical rotorcraft noise modeling method that accurately models the changes in rotor noise caused by maneuvering flight. Combinatoric optimization techniques are then employed to combine these maneuver segments into a low noise optimal flight path. A simple heuristic for estimating the total acoustic cost required to reach the target location is developed and incorporated into the search algorithm, allowing the computation of low noise paths in seconds. A procedure for implementing an "anytime" version of the method is described, enabling feasible solutions to be dynamically replanned "on the fly"—i.e., in fractions of a second—and refined over time to a low noise optimal solution.

INTRODUCTION

Community acceptance of rotorcraft operations is limited by the resulting noise. Voluntary restrictions on helicopter operations have recently been adopted in the Los Angeles and New York City areas (Refs. 1–3) in response to community objections to noise and the threat of legal restrictions on commercial operations. In addition to existing helicopter operations, proponents of Urban Air Mobility (UAM) foresee increases in rotorcraft operations in urban areas by orders of magnitude, but this goal is not achievable unless community acceptance of rotorcraft operations can be dramatically improved. Design changes can yield some reduction in rotor noise radiation, but usually with compromises in vehicle performance. However, due to the high sensitivity of rotorcraft noise to changes in rotor operating conditions, tailored noise abatement operations can be effective in reducing community noise impacts.

There exists a considerable body of work on low noise operations for rotorcraft. Much of this work has focused on avoiding Blade-Vortex Interaction (BVI) noise during approach using conventional optimization techniques (Refs. 4, 5). In many cases, the noise models underlying the optimization are only accurate for steady flight conditions (Ref. 6), and do not capture the significant changes in noise that can occur during transient maneuvers between steady flight states. This can lead to unrealistically low noise "optimal" approaches, for example, where the helicopter instantaneously transitions between shallow and steep descending flight conditions. The acoustic impacts of these trajectories are underpredicted because the transitions through the high BVI noise operating states between the shallow and steep descending flight conditions are not modeled. (Ref. 7).

Presented at the Vertical Flight Society 75^{th} Annual Forum, Philadelphia, PA, USA, May 13–16, 2019.

Even when realistically smooth flight conditions are appropriately modeled—including the acoustic effects of unsteady flight (Ref. 8)—computationally expensive optimization approaches are used (Refs. 9, 10), such that low noise operations must be planned well in advance of the actual flight.

The practicality of preplanned rotorcraft noise abatement operations is questionable because of ever-changing operational realities such as air traffic, weather, and unforeseen changes in mission objectives. Rapid trajectory planning and dynamic replanning have been long established and successfully applied in the field of robotics (Ref. 11), and more recently used to generate "on-the-fly" trajectories for Unmanned Aerial Vehicles (Ref. 12) and autonomous cars (Ref. 13). However, the cost functions applied in these approaches are typically much less computationally expensive than those necessary to accurately evaluate rotorcraft noise impacts. Although significant improvements in the computational efficiency of rotorcraft noise predictions have been realized recently (Ref. 14), developing near real time noise abatement guidance remains a challenge.

OBJECTIVE

The objective of this work is to develop a practical method of dynamic replanning for low noise rotorcraft operations with the following essential characteristics:

- physically-realizable and "flyable" transitions between vehicle flight states;
- accurate modeling of the dominant rotor noise sources, especially the sensitivity of radiated noise characteristics—frequency, magnitude, and direction—to changes in the rotor operating state; and
- rapid generation of low noise optimal flight trajectories—on the order of seconds—enabling practical "on-the-fly"

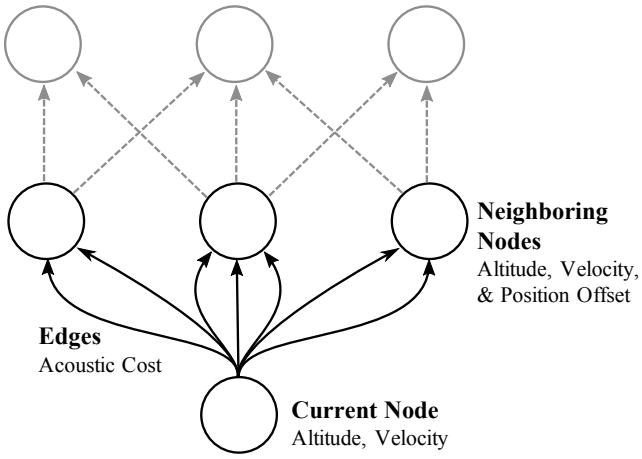

Fig. 1: Acoustic path planning graph.

replanning of low noise rotorcraft operations in response to changing circumstances.

TECHNICAL APPROACH

The basic concept of the approach developed in this work is that an entire rotorcraft operation can be represented by a sequence of fundamental maneuver segments that describe, in detail, how the vehicle transitions from one defined position and operating condition to another. Each segment can be evaluated offline to determine the overall "cost" of that portion of the flight trajectory according to its acoustic impact or any other metric of interest, such as time of flight, fuel consumption, or passenger comfort. This allows the trajectory optimization problem to be converted from a computationally expensive continuous optimization problem to the much cheaper combinatorial graph traversal, where the goal is to determine the lowest cost sequence of maneuver segments that connects the current position and state of the vehicle to the target position and state.

A diagram of the computational graph over which the low noise trajectory is generated is shown in Figure 1. Each maneuver segment connects from a particular flight state at the starting position to another flight state at some position offset from the starting position. In order to provide a physically realizable trajectory from the current vehicle position to the target position, the flight state at the end of each maneuver segment must match exactly that at the start of the next segment. In this paper, all segments begin and end in steady level flight, such that the vehicle is not accelerating at the points where the segments connect. The segment end points are then uniquely defined by their offset position (longitudinal and lateral) relative to the start point, change in heading, speed, and altitude above ground.

The space around the vehicle containing the target location is then populated by a grid of nodes, defined not only by their discrete position, but also by discrete altitudes, headings, and speeds. In this paper, the nodes are spaced 1000 m apart along Cartesian coordinates in X and Y, at altitudes from 50 m Above Ground Level (AGL) to 500 m AGL in 50 m increments, headings in 22.5 degree increments, and speeds from 20 m/s to 70 m/s in 10 m/s increments. The Y axis is defined to extend in the direction between the vehicle's starting position and the initial target location, and the X axis is along the ground perpendicular to this direction. The grid spans 40 nodes along the Y axis, and is 20 nodes wide along the X axis, covering an area of 800 km^2, approximately the same area as a moderately large city like Las Vegas, NV (741 km^2) or Austin, TX (824 km^2).

The connectivity between nodes is defined by the feasible set of maneuver segments, resulting in a graph containing all practical paths between the vehicle's current position and the target location. Figure 2 illustrates the range of nodes, shown as squares, that can be connected to the circular node shown in green. Nodes may be connected directly to nodes that are not immediate neighbors in physical space; for example, in this paper, nodes are connected by maneuver segments to their immediate neighbors—one grid spacing, Δx, apart and shown in magenta—as well as the next two concentric layers, shown in red and blue. Segments are also defined that connect all start and end node headings that are within 90 degrees of the line (shown dashed in Figure 2) connecting the start and end positions; i.e., segments may not start or end at a heading that opposes the overall direction of motion of the entire maneuver segment. Segments are defined that increase or decrease speed by 0, 10, 20, or 30 m/s, and altitude by 0, 50, 100, or 150 m.

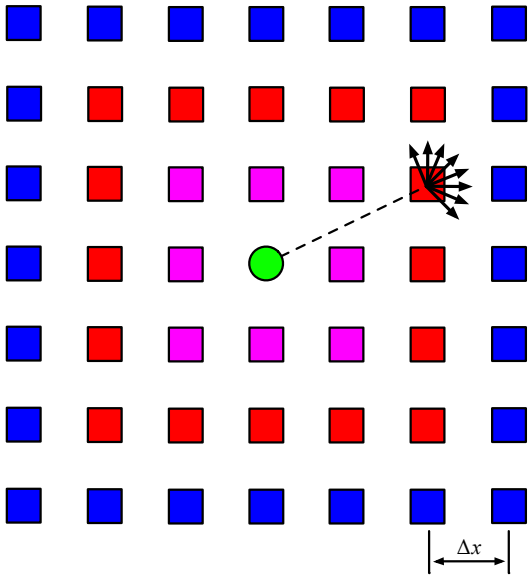

Fig. 2: An illustration of the connectivity of the circular node in green to nearby nodes, shown as magenta, red, and blue squares. The dashed line shows the direct path between the green node and one nearby node, and the arrows the admissible headings.

The detailed maneuver segment trajectories are uniquely defined by the cubic polynomials in time that connect the position and velocity of the starting node to the ending node. Altogether, over 300,000 different maneuver segments are available de-

scribing smooth and detailed trajectories, resulting in nearly 200 million edges that connect the approximately 500,000 nodes forming the graph. Each edge composing the graph is assigned a cost based on the detailed trajectory of the maneuver segment. These costs can be based on various acoustic or vehicle performance metrics, and can be varied with the location of the flight segment or emerging mission requirements. In this paper, only an acoustic cost is assigned to each of the 300,000 maneuver segments.

The acoustic cost of each maneuver segment is calculated using the FRAME-QS approach (Ref. 15), which is described in the flowchart shown in Figure 3. First, a semianalytical model of the helicopter's aerodynamics and acoustics is calibrated to measured acoustic data using the Fundamental Rotorcraft Acoustic Modeling from Experiments (FRAME) (Ref. 16) method. FRAME allows a limited set of measured noise data to be generalized across the entire range of rotor operating conditions a helicopter may enter during practical flight operations. The FRAME model is then used to build a database of acoustic spheres representing the magnitude and directivity of noise for a large number of rotor operating states. Measured broadband noise levels are simply interpolated from the measured data and added to the harmonic noise levels predicted by FRAME for each flight condition. The specific noise model used in this paper is derived from measurements of the Bell 407 helicopter collected during a joint NASA / FAA flight test in 2017 (Ref. 17), and consists of nearly 1000 acoustic spheres across the entire operating envelope of the helicopter.

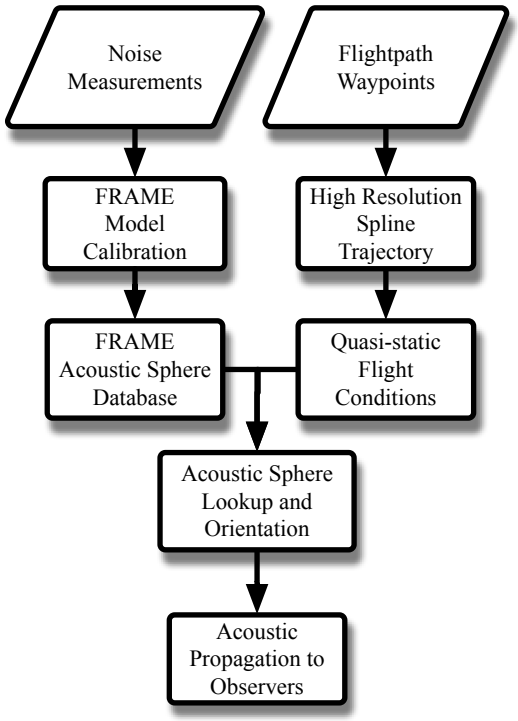

Fig. 3: A flowchart of the FRAME-QS maneuvering flight helicopter noise prediction method.

To predict the noise from a maneuver segment, a set of 10

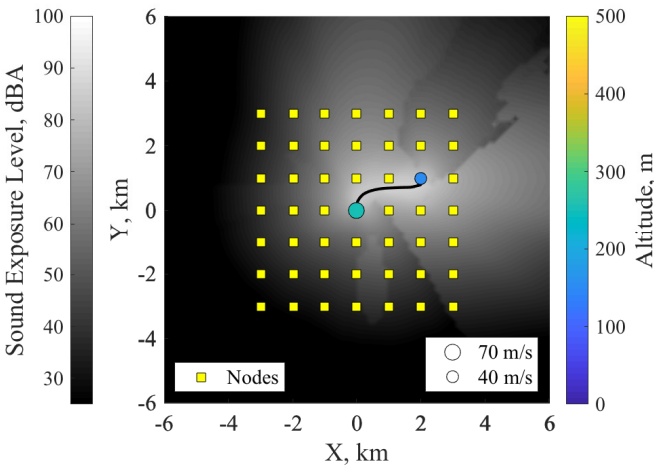

Fig. 4: Ground noise contours for a maneuver segment.

waypoints is determined using the cubic polynomial defining the maneuver segment. These waypoints are then interpolated to a high resolution flight trajectory using smoothing splines (Ref. 18). A simple point-mass flight dynamics model is used to predict the quasi-static rotor operating state and main rotor tip-path-plane orientation at each point along the trajectory. The rotor operating state and orientation are used to select a noise sphere from the database and orient it correctly for each point along the trajectory. At each point, the noise is propagated from the selected sphere to a grid of observers on the ground using a straight-ray method, including the effects of atmospheric absorption. The A-weighted Sound Pressure Levels (SPL) are integrated in time to calculate a Sound Exposure Level (SEL) at each point on the grid. Figure 4 shows an example of a maneuver segment. The helicopter begins at the circular marker at (X,Y) = (0,0) km, and travels along the black flight path to the marker at (X,Y) = (2,1) km. The spatial positions of all possible nodes reachable from the initial position are highlighted in yellow; this maneuver segment involves moving one node ahead of the vehicle's initial starting position and two nodes to the right. During the maneuver, the helicopter also descends from 200 m AGL to 50 m AGL, as denoted by the colors of the markers at the end points of the segments. The sizes of the markers represent the speed, where the helicopter decelerates from 70 m/s to 40 m/s. The resulting SEL ground noise level contours predicted by the FRAME-QS method for a maneuver segment are plotted in grayscale. This maneuver results in the generation of BVI noise—particularly during the aggressive turns at the beginning and end of the maneuver segment—which radiates most strongly toward the outside of the turns.

The SEL contours are then averaged over a 12 km square area—four times the area reachable from the center of the the area—to produce a single acoustic cost associated with that maneuver segment. This cost is assigned to each edge in the graph using this maneuver segment to connect between two nodes. Altogether, calculating the costs for all maneuver

segments used in this paper and constructing the graph took about 30 minutes of wall-clock computer time on a single 2.5 GHz Intel Core i7-E4870HQ Haswell CPU core. However, these computational costs need only be incurred once, as the graph, once constructed, can be stored in memory and modified nearly instantaneously to represent changing circumstances. For instance, edges between nodes can be marked as invalid to represent airspace that is no longer available, and the costs associated with each segment can be updated to represent the acoustic sensitivity of the position of the node or re-weighted to prioritize non-acoustic objectives, such as minimizing fuel costs. The graph used in this paper takes 3.9 GB of memory to store; the same information may be expressed in significantly less space—perhaps tens of MB—as no consideration was given to the efficient use of memory in the low noise dynamic replanning computer program created for this paper.

Numerous algorithms have been developed to find the lowest cost path between two nodes on a graph. One of the most well-known is Dijkstra's algorithm (Ref. 19), a special case of the "greedy" best-first search, that can identify the lowest cost path between two nodes. Dijksta's algorithm expands outward from the starting node, and explores all neighboring nodes that are closer to the destination, updating the shortest possible path as it progresses.

An accelerated variant of the algorithm, called A* search[1] (Ref. 20), employs a heuristic to guide the search. The heuristic should represent an "optimistic" lower bound cost between any node and the destination; if the A* algorithm has already found a path from the starting node to the target node, it can ignore all nodes where the heuristic is greater than the cost of the identified path, since the true paths of those nodes must cost at least as much. The heuristic used in this work can be expressed as:

$$h(n) = \bar{L}_{ae_{min}} \frac{\|(x - x(n))^2 + (y - y(n))^2\|}{\Delta x} \qquad (1)$$

where, $\bar{L}_{ae_{min}}$ is the lowest acoustic cost in the database of maneuver segments, Δx is the grid spacing along the ground plane (1 km), $x(n)$ and $y(n)$ are the X and Y coordinates of the node being evaluated, x and y the coordinates of the target. This formulation guarantees that the heuristic will be an "optimistic" estimate of any real path traversing through that node, since the actual path can be no shorter than the Euclidean distance between the target and the node and the acoustic cost for each grid space, Δx, traversed must always be at least the minimum cost, $\bar{L}_{ae_{min}}$.

A* can further be accelerated by overweighting the heuristic by some factor, such that it is no longer "optimistic" (Ref. 21). The overweighted heuristic can then be expressed as:

$$h_\varepsilon(n) = \varepsilon h(n) = \varepsilon \bar{L}_{ae_{min}} \frac{\|(x - x(n))^2 + (y - y(n))^2\|}{\Delta x} \qquad (2)$$

where ε is the amount of overweighting.

Overweighting the heuristic causes A* to search fewer nodes, improving computational performance at the expense of the optimality of the resulting solution. However, the total cost of the solution found is still guaranteed to be no more than ε times greater than the optimal path. This ability to trade off optimality for computational efficiency allows A* to be used as an "anytime" algorithm, by beginning the search with a highly inflated heuristic and incrementally decreasing the weight of the heuristic value to achieve more accurate results until either the optimal (unweighted) solution is achieved or a bounded amount of time has elapsed, guaranteeing that some solution will be available within the allowable time interval. The A* algorithm is used in this work to find the lowest cost path between nodes in the graph, and therefore, a low noise path between the vehicle's location and the target position.

[1] Pronounced "A star," but unrelated to the homonymous helicopter.

RESULTS

Low Noise Optimal Flight Planning

Figure 5 shows an example of applying the method described in the previous section to a low noise path planning problem. The path is plotted using the same symbology as Figure 4 from the previous section. The colored rectangle represents closed airspace starting at an altitude above ground level indicated by the color and extending upwards; i.e., the blue rectangle represents closed airspace at all altitudes. The helicopter begins just after takeoff at 50 m altitude and 20 m/s speed at (X,Y) = (10,0) km and flies 40 km in the Y direction ending in the same 50 m AGL, 20 m/s flight condition at the terminal area. The helicopter initially turns to a heading directed away from the obstacle on the left side of the plot while at low speed and altitude, to minimize the acoustic effect of the turns. The helicopter then accelerates and climbs to reduce the noise levels directly under the flight path, changing heading again only after reaching an altitude of 400 m. The descent is then maintained at constant speed until the vehicle is low to the ground, at which point the speed is reduced. This solution is the lowest acoustic cost path through the graph. Using Djikstra's algorithm, the optimal path takes 870 seconds of wall clock time to compute on a single 2.5 GHz Intel Core i7-E4870HQ Haswell CPU core, representing 1058 seconds of flight time. Incorporation of the A* heuristic accelerates the computation greatly: the same optimal path is computed in 40.5 seconds, which is less than the shortest time it takes to traverse from one node of the planned trajectory to another (44.5 s).

Replanning

The low noise trajectory can be quickly replanned in response to changes in the environment. In this section, all trajectories will be replanned from the same starting location, (X,Y) = (10,0) km, as the case shown in Figure 5 for ease of comparison, but in practice, the trajectories can be replanned starting at any point along the flight path.

Figure 6 shows the optimal solution when the obstacle is re-located to the right side of the flight path. The optimal flight path has similar features to that of the original flight path, with the noisier turning flight segments performed either at high

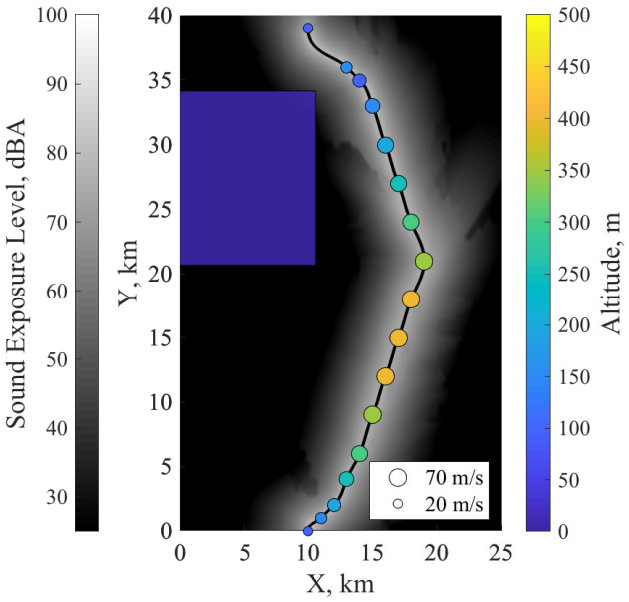

Fig. 5: Optimal path with obstacle on the left.

altitude or while at low speed in the takeoff and landing areas of the flight trajectory. The A* search is further accelerated to 29.4 seconds by exploiting previously cached information about the acoustic costs of traversing from one node to another.

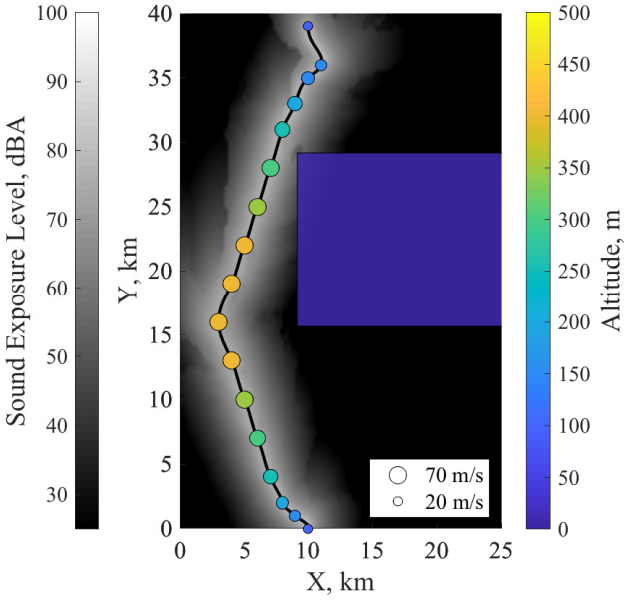

Fig. 6: Optimal path with obstacle on the right.

The airspace available to rotorcraft operations is often limited to below a ceiling, due to weather or the operations of less maneuverable fixed wing aircraft in the vicinity of an airport. For example, Figure 7 shows the replanned trajectory when an additional altitude restriction is applied at 200 m, representing vertical separation with the approach or departure corridor of a fixed-wing aircraft. This forces the helicopter to fly at a lower altitude to get below the corridor, increasing noise levels directly underneath the flight path. The ground track of the path is otherwise similar to that shown in Figure 6. Once again, replanning is more efficient due to previously cached information, with the A* search taking 26.8 seconds to complete.

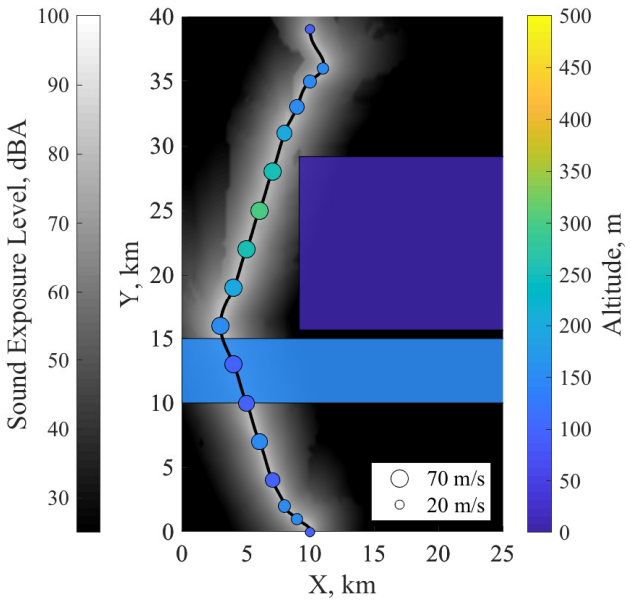

Fig. 7: Optimal path with obstacle on the right and altitude restriction.

Due to the varied nature of the missions performed and the uncontrolled nature of most low-altitude airspace, rotorcraft operations are often planned in an ad hoc manner, with objectives that change "on the fly." Figure 8 shows a trajectory planned where the target landing zone has been moved to (X,Y) = (20, 35) km. The low noise optimal solution, planned in 29.7 seconds, adds an additional low altitude turn to provide more time to gradually decelerate to the new terminal area.

"Anytime" Dynamic Replanning

Although the A* algorithm can replan low noise flight paths much faster than conventional methods, even faster planning of feasible low noise solutions may be required when generating new trajectories "on the fly," e.g., when the rotorcraft departs from the originally planned course. As mentioned in the previous section, faster solutions may be obtained from the A* method by overweighting the heuristic. This restricts the search space, reducing the time required to compute a path at the expense of optimality. Figure 9 shows the path obtained when overweighting the heuristic to 110% of the nominal value for the same scenario as Figure 6.

The resulting path is essentially the same as that shown in Figure 6, but the computational time required to replan the trajectory was reduced from 29.4 seconds to 10.3 seconds. Further speedups are possible by further overweighting the

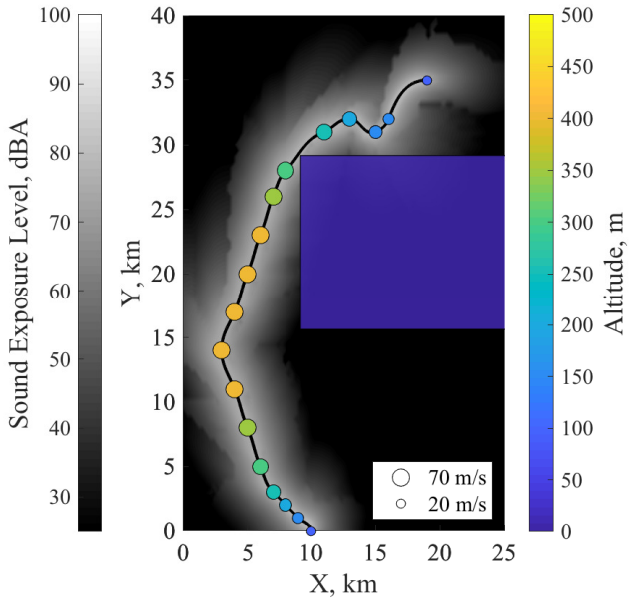

Fig. 8: Optimal path with obstacle on the right and new target location.

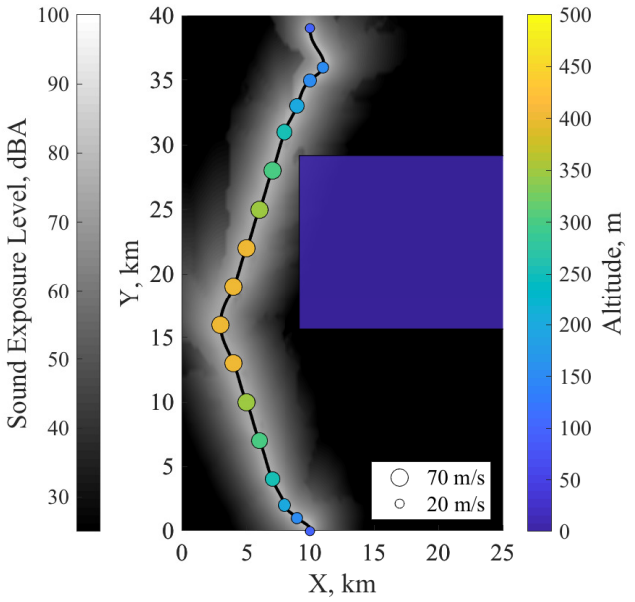

Fig. 9: "Anytime" path with 110% overweighting for obstacle on right.

heuristic. Figure 10 shows the result when the heuristic is overweighted 125%. The resulting path is feasible, but diverges somewhat from the optimum. Not as much of the high speed portion of the path occurs at high altitudes, and several unnecessary turns are incorporated, increasing the SEL observed toward the outside of the turns. However, the computational time required to dynamically replan is reduced to 3.4 seconds.

Figure 11 shows the path dynamically replanned repeated with 150% overweighting. This path is similar to the 125% case shown in Figure 10, but was computed in only 1.2 seconds. Finally, Figure 12 shows the path resulting from 200% overweighting. The optimality of the solution is further compromised, with maneuver induced BVI noise setting noise levels near the terminal area of the trajectory, but a feasible trajectory is achieved in 250 ms.

These results illustrate how an effective "anytime" dynamic replanner can be constructed using the A* algorithm. When replanning is required, multiple A* solvers can be launched, either in series from the highest overweighting to no overweighting, or preferably, in parallel. In less than one second, some feasible path can be generated with a heavily overweighted heuristic. As the computation continues and solutions are reached with less overweighing, the path is refined until it reaches the low noise optimal solution.

Handling Qualities Implications

As the heuristic value is inflated to enable the more rapid generation of paths, the resulting trajectories tend to include more frequent and aggressive maneuvers due, in part, to the discretization enforced by the graph. This raises concerns about the pilot workload required to track these trajectories. Following the methods developed in Hess, Zeyada, and Heffley

Table 1: Estimated pilot crossover frequencies (rad/s) for trajectories generated with different levels of A* heuristic overweighting, ε.

ε	100%	110%	125%	150%	200%
Pitch	1.12	1.12	1.26	2.00	2.40
Roll	1.20	1.20	1.37	1.59	1.33
Yaw	0.150	0.150	0.443	0.687	0.983
Heave	0.0037	0.0037	0.0023	0.0024	0.0024

(Ref. 22), the inner-loop crossover frequencies that must be employed by the pilot to maneuver the helicopter along these trajectories can be estimated as:

$$\omega_B = 2.4 \frac{\Delta\dot{\phi}_{max}}{\Delta\phi_{max}} \quad \text{(rad/s)} \tag{3}$$

where $\Delta\phi_{max}$ is the maximum change of pitch, roll, yaw, or heave, and $\Delta\dot{\phi}_{max}$ is the maximum rate of change of pitch, roll, yaw, or heave over the entire trajectory. The resulting crossover frequencies, ω_B, along each axis are shown in Table 1, for each of the trajectories generated at different heuristic overweighting factors, ε, shown in the previous section.

The required inner-loop crossover frequencies highlight the the large pitch and yaw rates required to fly these trajectories, especially at the higher levels of ε, 150% and 200%, where unnecessarily aggressive changes in speed and heading will require high levels of pilot workload.

CONCLUSIONS

This paper demonstrates the existence of a feasible dynamic replanning method for generating practical low noise rotorcraft flight trajectories "on the fly." The method incorporates accurate rotorcraft noise modeling, which realistically accounts

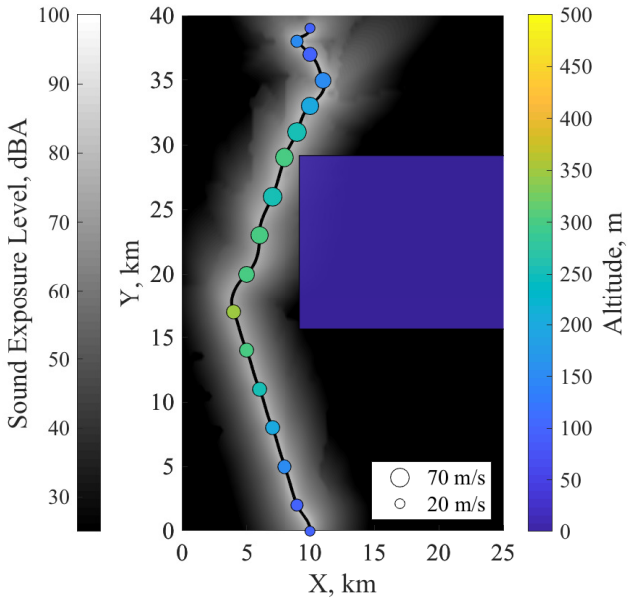

Fig. 10: "Anytime" path with 125% overweighting for obstacle on right.

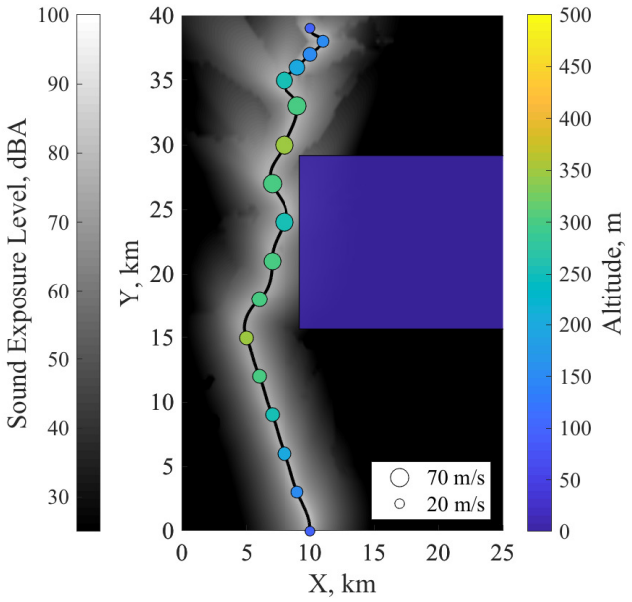

Fig. 11: "Anytime" path with 150% overweighting for obstacle on right.

for the changes in noise caused by maneuvering flight during transitions between steady flight segments, accounting for the particular sensitivity of rotorcraft noise to changes in rotor operating condition. A heuristic was developed to enable rapid low noise trajectory generation using the A* search algorithm. Further speed increases were demonstrated through overweighting of the heuristic, enabling an "anytime" version of the algorithm to be employed. However, excessive overweighting yielded trajectories that are likely very demanding for pilots to fly, suggesting that handling qualities constraints should be imposed on the overweighted solutions. This method is suitable for generating "on the fly" noise abatement guidance for crewed rotorcraft and to effectively incorporate acoustic considerations into the operations of autonomous rotorcraft.

Future Research Directions

This paper demonstrates that dynamic replanning of low noise rotorcraft flight trajectories is possible using a combinatorial optimization approach. Further research is required to identify the most effective, least computationally expensive, and most useful implementation of this concept. Some research directions leading toward this goal include:

- The trajectories shown in this paper were developed using only acoustic considerations; however, the cost of traversing from one node to another can be determined by any number of factors. Other important factors should be considered in the future, such as flight time or fuel consumption, in addition to noise. Maneuver costs based on noise could be heavily weighted in noise sensitive areas, while performance considerations are more heavily weighted in regions where noise is less important.
- Flight guidance, navigation, and control considerations should be considered in any practical implementation of this approach because the generated trajectories can impose demanding maneuver requirements. Even for fully autonomous vehicles, ride quality considerations are still a concern when passengers are on board. Depending on the type of mission being flown, different constraints could be imposed on the aggressiveness of maneuvers.
- The resulting trajectories are limited to certain paths due to the limited number of precomputed trajectory segments. This can result in paths where the flight condition of the vehicle is continuously varying, for example when the desired heading to the target does not match one of the discrete headings defined at each maneuver node. It is this discretization that is responsible for much of the complexity of the resulting trajectories. Instead of using the trajectory segments directly, the precomputed database of noise results could be used to inform an empirical model that could generate a specific noise cost for a trajectory generated "on the fly." This would permit alternative search algorithms to be used, such as θ^* (Ref. 23), that enable direct connectivity between any pair of nodes on the graph. Such an approach would result in smoother and more effective trajectories, and most likely, a further increase in computational efficiency of the method.
- Algorithmic improvements may enable faster path generation with greater potential noise reductions. For example, a hybrid method might use inexpensive empirical models or precomputed templates to identify potentially promising low noise paths, and then perform a more detailed assessment of the best performing candidates with a more computational expensive, but still faster-than-real-time, simulation model. Recent research in combinatorics has

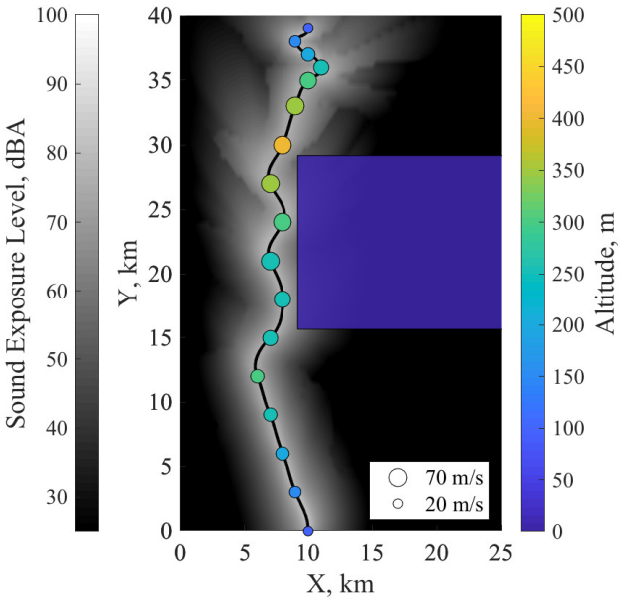

Fig. 12: "Anytime" path with 200% overweighting for obstacle on right.

shown that probabilistic algorithms (Ref. 24) often have excellent performance on a variety of graph traversal problems, especially when there may be multiple objectives to optimize, e.g., noise and performance.

ACKNOWLEDGMENTS

The author thanks Dr. Carlos A. Malpica, NASA Ames Research Center, for his guidance on evaluating the "flyablility" of the generated low noise trajectories and insights on interpretation of the results. The author also thanks Ms. Anna C. Trujillo, NASA Langley Research Center, and Dr. James H. Stephenson, US Army, for many helpful discussions on practical approaches to low noise path planning during the preparation of this paper.

Author Contact

Eric Greenwood
eric.greenwood@nasa.gov

REFERENCES

[1]"LA Helicopter Noise Initiative," http://heli-noise-la.com, Accessed: 2017-03-05.

[2]"Westchester County Airport Noise Abatement," http://airport.westchestergov.com/environmental-management-system/noise-abatement, Accessed: 2017-03-05.

[3]"NYCEDC And Helicopter Tourism & Jobs Council Announce New Measures to Reduce Helicopter Noise And Impacts Across New York City," https://www.nycedc.com/press-release/nycedc-and-helicopter-tourism-jobs-council-announce-new-measures-reduce-helicopter, Accessed: 2017-03-05, February 2016.

[4]Padula, S. L., Burley, C. L., Boyd Jr, D. D., and Marcolini, M. A., "Design of Quiet Rotorcraft Approach Trajectories," Technical Report TM-2009-215771, NASA, 2009.

[5]Cruz, L., Massaro, A., Melone, S., and D'Andrea, A., "Rotorcraft Multi-Objective Trajectory Optimization for Low Noise Landing Procedures," 38th European Rotorcraft Forum, 2012.

[6]Morris, R., Johnson, M., Venable, K. B., and Lindsey, J., "Designing Noise-Minimal Rotorcraft Approach Trajectories," *ACM Trans. Intell. Syst. Technol.*, Vol. 7, (4), April 2016, pp. 58:1–58:25.

[7]Gopalan, G., Xue, M., Atkins, E., and Schmitz, F. H., "Longitudinal-Plane Simultaneous Non-Interfering Approach Trajectory Design for Noise Minimization," American Helicopter Society 59th Annual Forum, May 2003.

[8]Greenwood, E., "Helicopter Flight Procedures for Community Noise Reduction," American Helicopter Society 73rd Annual Forum, May 2017.

[9]Guntzer, F., Spiegel, P., and Lummer, M., "Genetic Optimizations of EC-135 Noise Abatement Flight Procedures using an Aeroacoustic Database," 35th European Rotorcraft Forum, September 2009.

[10]Hartjes, S. and Visser, H., "Optimal Control Approach to Helicopter Noise Abatement Trajectories in Nonstandard Atmospheric Conditions," *Journal of Aircraft*, Vol. Article in Advance, 2018, pp. 1–10.

[11]Brumitt, B. L. and Stentz, A., "Dynamic mission planning for multiple mobile robots," Proceedings of IEEE International Conference on Robotics and Automation, Vol. 3, April 1996.

[12]De Filippis, L., Guglieri, G., and Quagliotti, F., "Path Planning Strategies for UAVS in 3D Environments," *Journal of Intelligent & Robotic Systems*, Vol. 65, (1), Jan 2012, pp. 247–264.

[13]Li, X., Sun, Z., Cao, D., Liu, D., and He, H., "Development of a new integrated local trajectory planning and tracking control framework for autonomous ground vehicles," *Mechanical Systems and Signal Processing*, Vol. 87, Signal Processing and Control challenges for Smart Vehicles, 2017, pp. 118 – 137.

[14]Greenwood, E., "Real Time Helicopter Noise Modeling for Pilot Community Noise Awareness," *INTER-NOISE and NOISE-CON Congress and Conference Proceedings*, Vol. 254, (2), 2017, pp. 372–380.

[15]Greenwood, E., Rau, R., May, B., and Hobbs, C., "A Maneuvering Flight Noise Model for Helicopter Mission Planning," American Helicopter Society 71st Annual Forum, May 2015.

[16]Greenwood, E. and Schmitz, F. H., "A Parameter Identification Method for Helicopter Noise Source Identification and Physics-Based Semiempirical Modeling," *Journal of the American Helicopter Society*, Vol. 63, (3), 2018, pp. 1–14.

[17]Watts, M. E., Greenwood, E., Stephenson, J. H., and Smith, C. D., "Noise Abatement Flight Test Data Report," Technical Report TM-2019-220265, NASA, March 2019.

[18]Reinsch, C. H., "Smoothing by Spline Functions," *Numerische Mathematik*, Vol. 10, (3), October 1967, pp. 177–183.

[19]Dijkstra, E. W., "A note on two problems in connexion with graphs," *Numerische Mathematik*, Vol. 1, (1), December 1959, pp. 269–271.
[20]Hart, P. E., Nilsson, N. J., and Raphael, B., "A Formal Basis for the Heuristic Determination of Minimum Cost Paths," *IEEE Transactions on Systems Science and Cybernetics*, Vol. 4, (2), July 1968, pp. 100–107.
[21]Likhachev, M., Ferguson, D., Gordon, G., Stentz, A., and Thrun, S., "Anytime Dynamic A*: An Anytime, Replanning Algorithm," Proceedings of the International Conference on Automated Planning and Scheduling (ICAPS), 2005.
[22]Hess, R. A., Zeyada, Y., and Heffley, R. K., "Modeling and Simulation for Helicopter Task Analysis," *Journal of the American Helicopter Society*, Vol. 47, (4), October 2002, pp. 243–252.
[23]Daniel, K., Nash, A., Koenig, S., and Felner, A., "Theta*: Any-angle path planning on grids," *Journal of Artificial Intelligence Research*, Vol. 39, 2010, pp. 533–579.
[24]Bossek, J. and Grimme, C., "Solving Scalarized Subproblems within Evolutionary Algorithms for Multi-Criteria Shortest Path Problems," International Conference on Learning and Intelligent Optimization, 2018.